

# A New Angular Tropospheric Refraction Model

A. L. Berman and S. T. Rockwell<sup>1</sup>  
Network Operations Office

*As part of an effort to obtain a new angular tropospheric refraction model for use within the DSN, an empirical model has been constructed which very accurately reflects precise optical refraction data. The model developed is a single analytic function, is finite over the entire domain of elevation angle, and is highly accurate over large ranges of pressure and temperature.*

## I. Introduction

There exists here at the Jet Propulsion Laboratory (JPL), and particularly within the Deep Space Network (DSN), a need for an accurate, yet modestly sized, angular tropospheric refraction model. The basic angular refraction model (and several close variants) currently in use at JPL consists of three radically different analytic functions, each applicable over a different range of zenith angle (zenith angle =  $90^\circ - \text{elevation angle}$ ) and is therefore immediately rather cumbersome. Furthermore, the accuracy of the current JPL refraction model is not well documented, and is thus subject to considerable doubt.

The present time is particularly well suited to reexamine the question of an angular refraction model for the following reasons:

- (1) The remote site Antenna Pointing Subsystem (APS) is currently being redesigned, thus affording the capability to easily change the angular refraction modeling.
- (2) The recent advent of X-band capability, with an antenna beamwidth of approximately  $0.020^\circ$ , has underscored the need for high-accuracy angular predicts.

The angular refraction model (or variants thereof) currently in use at JPL is as follows:

- (1) For  $Z \leq 80.26^\circ$ ,

$$R = (N/10^6) \tan Z$$

- (2) For  $90^\circ \geq Z > 80.26^\circ$ ,

$$R = \left( \frac{N}{340} \right) \left( \frac{0.0007}{0.0589 + \left( \frac{\pi}{2} - Z^* \right)} - 0.00126 \right)$$

<sup>1</sup>Currently graduate student in physics at the University of California at Los Angeles.

(3) For  $Z > 90^\circ$ ,

$$R = \left(\frac{\pi}{180}\right) \left(0.60874 - 0.201775 \left\{\frac{180}{\pi}\right\} \left[Z^* - \frac{\pi}{2}\right]\right)$$

where

$R$  = refraction correction, rad

$Z$  = zenith angle (actual), deg

$Z^*$  = zenith angle (actual), rad

$N$  = "refractivity"

To gauge the degree of error inherent to the current JPL refraction model, it has been contrasted to a continuous set of refraction data as computed from the work of B. Garfinkel (see Refs. 1 and 2), and is seen in Fig. 1. The Garfinkel data is for pressure  $P = 760$  mm of Hg and temperature  $T = 0^\circ\text{C}$ ; the JPL model data has been matched to these conditions by setting  $N = 288$ . The most distressingly obvious flaws in the current JPL model are the discontinuities in  $R$  at the two breakpoints, these discontinuities (and hence errors in one or the other segment) amounting to approximately 30 and 300 arc seconds (sec), respectively. (Note: For the duration of this report, refraction quantities will be dealt with in terms of arc seconds, with  $0.001^\circ = 3.6$  sec.) Further examination of the current model discloses that the first two segments are dependent upon the "refractivity"  $N$ , and hence pressure and temperature, while the third segment is not. Given that the current JPL model is inaccurate, has very large discontinuities at the segment breakpoints, and is fundamentally cumbersome because of the tri-segment construction, it would seem to be a likely candidate for a more accurate and reasonable replacement.

## II. General Approach to a New Angular Refraction Model

In the previous section, the undesirability of the current JPL angular refraction model was demonstrated; in this section the general philosophy used to generate a new angular refraction model will be dealt with. One starts with the fact that angular refraction is crucially important in the effectuation of various astronomical endeavors, and hence there exists copious amounts of refraction data. The main drawback to these data is, however, that they are either in tabular form or are calculated via schemes which require large amounts of tabular inputs (for instance, see Refs. 1, 2, 3, and 4). Furthermore, the astronomical accuracy requirements are very stringent (perhaps down to about the 1-sec level), while the DSN

requirements are no greater than the 10-sec level. In light of the above, it is clear that one reasonable approach would be to use empirical methods to develop a simple analytical expression to approximate the very accurate astronomical refraction data available. Since the envisioned use of the new model within the DSN includes small remote site computers as well as large central complex computers, desirable features would include:

- (1) A single expression over the entire domain of  $Z$ , instead of multiple segments, each applicable over different ranges of  $Z$ .
- (2) Accuracy to about the 10-sec level for reasonable ranges of  $Z$  and tropospheric conditions.
- (3) Model to be designed to minimize both computer memory and run time.

## III. Selection of an Angular Refraction Data Base

After a review of the literature, it became apparent that a reasonable selection for a data base would be the work of Boris Garfinkel of the Yale University Observatory (see Refs. 1 and 2). Garfinkel's original theory was published in 1944, and then reexamined in 1966. The form of his model is semi-analytical in that it is a closed function with  $Z$ ,  $P$ ,  $T$  as variables, but also requires tabular input in the form of  $Z$ -dependent polynomial coefficients. More importantly, his model is continued for  $Z > 90^\circ$ , an aspect which is most frequently missing in other angular refraction works. Finally his work compares well with other authorities in the field. For instance, Garfinkel compares his data at  $P = 760$  mm and  $T = 0^\circ\text{C}$  with those of the Radau and the Pulkova models as follows (with  $Z'$  (observed zenith angle) in degrees and  $R$  in seconds):

$Z'$	$R$ Garfinkel	$R$ Radau	$R$ Pulkova
80	331	331	331
81	368	366	365
82	410	409	408
83	463	462	460
84	531	529	527
85	619	617	614
86	738	735	733
87	905	903	900
88	1153	1152	1147
89	1544	1545	1537
90	2206	2208	2199

Table 1 provides a detailed tabulation of Garfinkel refraction data for  $0^\circ \leq Z \leq 93^\circ$ ,  $P = 760$  mm, and  $T = 0^\circ\text{C}$ .

#### IV. Derivation of a Basic Angular Refraction Model

The needs of the DSN for an angular refraction model are restricted to the following range of  $Z'$ :

$$0^\circ \leq Z' \lesssim 92^\circ$$

where

$$Z' = Z - R(Z) = \text{observed zenith angle}$$

this range being encompassed by the Garfinkel data in Table 1. It was hoped that the data base chosen (i.e., the Garfinkel data whose selection was discussed in the previous section) could be approximately fit to a function (or functions, as necessary) via routine least squares techniques. It was planned to do all work for  $P = 760$  mm and  $T = 0^\circ\text{C}$  under the assumption that  $P$  and  $T$  effects could be (multiplicatively) added at a subsequent time. The data base chosen was a slightly smaller subset of the data base displayed in Table 1. The frequency of data points was rather arbitrarily chosen as follows:

Range of $Z$ , deg	Data frequency, deg
$0 \leq Z \leq 70$	0.5
$70 \leq Z \leq 85$	0.2
$85 \leq Z \leq 93$	0.1

with the net effect that the refraction data were increasingly "weighted" in the high  $Z$  region where the rate of change of refraction is the greatest. The computer program utilized in this study is a standardized least squares subroutine available to all UNIVAC 1108 users at JPL (see Ref. 5). Basically, it fits a data set to an  $n$ th degree polynomial such that the residuals are minimized in a least squares sense, i.e.,

$$\text{if } R_i(Z_i); \quad i = \text{data set}$$

then a function  $X$  is formulated such that

$$X = \sum_{j=0}^n K_{j+3} \{U(Z)\}^j$$

where

$$K_1 = \frac{1}{2} [(R_i)_{\max} + (R_i)_{\min}]$$

$$K_2 = \frac{1}{2} [(R_i)_{\max} - (R_i)_{\min}]$$

$$U(Z) = \frac{1}{K_2} [Z - K_1]$$

and where the conditions satisfied are the following  $n$  equations in  $n$  unknowns.

Let

$$\Delta_i = R_i(Z_i) - X(Z_i)$$

$$\sigma = \left[ \sum \Delta_i^2 \right]^{1/2}$$

Then, finally,

$$\frac{\partial \sigma}{\partial K_3} = 0$$

$$\frac{\partial \sigma}{\partial K_4} = 0$$

.

$$\frac{\partial \sigma}{\partial K_{j+2}} = 0$$

It was originally intended to attempt a least squares curve fit to the "raw" refraction data, shown in Fig. 2. It was observed, however, that the natural log (ln) of  $R$  gave a very smooth representation and possessed, of course, far less dynamic range, as can be seen in Fig. 3. It seemed possible that it might yield a better fit for a lower order polynomial (a desirable property), i.e., fitting:

$$\ln(R_i(Z_i)); \quad X$$

Finally, it was observed that taking the inverse tangent (arctan) of  $\ln(R)$  yielded a representation that appeared almost linear, as can be seen in Fig. 4. This was also felt to be worth attempting as a fit, in the form of:

$$\arctan \left\{ \frac{\ln(R_i(Z_i))}{\ln(R(45^\circ))} \right\}; \quad X$$

The  $\ln(R)$  fit was attempted first as the most likely candidate. The main goal established was to find the smallest order fit which would keep the maximum residual below some reasonable limit. The results of a series of different order fits appear in Fig. 5. Although it might at first seem strange that the absolute maximum residual does not decrease monotonically with degree of fit, all one should really expect is that  $\sigma$  decrease monotonically with degree of fit, and this was the case. At any rate, the 8th degree case was felt to be the best compromise, as one needed to go to a 14th degree fit to obtain significant improvement. The other two types of fits were attempted, with a general tradeoff expected that an increase in functional dependence ( $\ln$ ,  $\arctan$ , etc.) should decrease the order of fit necessary. A few of the salient features of each of the three types of fits attempted are:

(1) Raw Data Fit

- (a) Simple—no additional functions required for modeling.
- (b) Minimum acceptable polynomial required  $\sim 12$ th order.
- (c) Large residuals ( $\sim 20$  sec or higher) as  $Z \rightarrow 0^\circ$ , leading to unpalatable result of refraction being applied in wrong direction at very small  $Z$ , etc.

(2)  $\ln(R)$  Fit

- (a) Model would require natural exponentiation ( $\exp$ ).
- (b) Minimum acceptable polynomial required  $\sim 8$ th order.
- (c) Logarithmic condition of fit forces residuals to be approximately proportional to  $R$ , so residuals quite small except at very large  $Z$ .

(3)  $\arctan(\ln(R))$  Fit

- (a) Model would require tangent ( $\tan$ ) and  $\exp$ .
- (b) Minimum polynomial fit required  $\sim 6$ th order.
- (c) Extremely low residuals for  $Z \lesssim 90^\circ$  and quite high residuals for  $Z \gtrsim 90^\circ$ .

A comparison of the three types of fits is seen in Fig. 6.<sup>2</sup> The  $\ln R$  fit was assessed to be the best compromise

<sup>2</sup>This figure and Figs. 7, 9, and 10 were prepared on the basis of interim results and are at variance with the final model by as much as 5 sec at large  $Z$ . Therefore, they should be used for illustration only.

amongst the design goals stated in Section II. Further refinement to the 8th order  $\ln R$  fit was accomplished by making minor adjustments to the data set used in the fit process, until an optimum fit (in the sense of the smallest maximum residual) was achieved. For this case, the maximum residual in the interval  $0^\circ \leq Z \leq 92^\circ$  occurred at about  $Z = 91.1^\circ$  and had a value of:

$$\Delta R = +21.6 \text{ sec}$$

## V. Complete Refraction Model Determination

The refraction model, as finally determined in the previous section, is as follows:

$$R = \exp \left\{ \sum_{j=0}^8 K_{j+3} [U(Z)]^j \right\} - K_{12}$$

where

$R$  = refraction, sec

$Z$  = zenith angle, actual

$EL = 90^\circ - Z$  = elevation angle

$$U(Z) = \left\{ \frac{Z - K_1}{K_2} \right\}$$

$$K_1 = 46.625$$

$$K_2 = 45.375$$

$$K_3 = 4.1572$$

$$K_4 = 1.4468$$

$$K_5 = 0.25391$$

$$K_6 = 2.2716$$

$$K_7 = -1.3465$$

$$K_8 = -4.3877$$

$$K_9 = 3.1484$$

$$K_{10} = 4.5201$$

$$K_{11} = -1.8982$$

$$K_{12} = 0.89000$$

When this model is compared to the Garfinkel data (with  $P = 760$  mm and  $T = 0^\circ\text{C}$ ), the following maximum residuals<sup>3</sup> result:

$$0^\circ \leq Z \leq 85^\circ \quad \Delta R = + 5.6 \text{ sec}$$

<sup>3</sup>All residuals ( $\Delta R$ ) will be Garfinkel Data — Proposed Model.

$$85^\circ \leq Z \leq 92^\circ \quad \Delta R = + 21.6 \text{ sec}$$

$$92^\circ \leq Z \leq 93^\circ \quad \Delta R = -302.6 \text{ sec}$$

The very large residuals between  $Z = 92^\circ$  and  $Z = 93^\circ$  are primarily a result of ending the fit at  $92^\circ$ . At this point there was still one point of concern and that was:

As  $Z > 93^\circ$

$|R| \rightarrow \text{very large}$

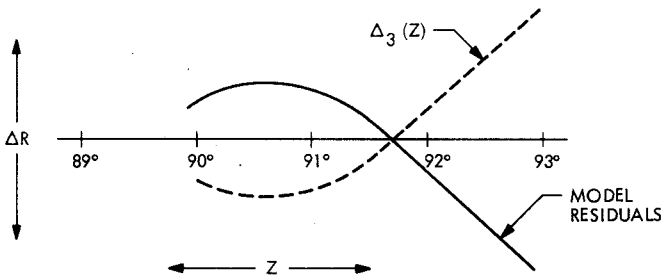
such that at some  $Z > 93^\circ$  there exists the following condition:

$$Z - R(Z) < 90^\circ \text{ (or local horizon)}$$

giving the appearance of a "false" rise. This would, of course, pose difficulties for trajectory-type programs which calculate, and examine for a rise condition, zenith angles considerably larger than  $90^\circ$ . Based on this undesirable feature, it was felt that the model should be modified such that shortly after  $Z = 93^\circ$  it would be required that:

$$R(Z) \rightarrow 0$$

At the same time, it was felt that possibly the characteristics of the model for  $Z \gtrsim 90^\circ$  could be improved upon. The residuals between  $Z = 90^\circ$  and  $Z = 93^\circ$  look like:



It was therefore felt that if a function (say,  $\Delta_3(Z)$ ) could be derived with inverse characteristics to the above residuals plus possessing the following qualities:

$$\Delta_3(Z) \rightarrow \text{very large for } Z \gtrsim 93^\circ$$

$$\Delta_3(Z) \rightarrow \text{very small for } Z \lesssim 90^\circ$$

Then a model of the form:

$$R = \exp \left\{ \left( \sum_{j=0}^8 K_{j+3} [U(Z)]^j \right) / [1 + \Delta_3(Z)] \right\} - K_{12}$$

could perhaps both improve the present model between  $90^\circ$  and  $93^\circ$  and drive the model to approximately zero (actually  $1 - K_{12}$ ) thereafter. A function to accomplish this was constructed (empirically) as follows:

$$\Delta_3(Z) = (Z - C_0) \{ \exp [C_1(Z - C_2)] \}$$

where

$Z$  = zenith angle, deg

$$C_0 = 91.870$$

$$C_1 = 0.80000$$

$$C_2 = 99.344$$

The improvement in the  $Z = 90^\circ$  to  $Z = 93^\circ$  region can be seen in Fig. 7, while the rapid drop off of the modified model after  $Z = 93^\circ$  can be viewed in Fig. 8. The maximum residuals after the above modification become:

$$0^\circ \leq Z \leq 85^\circ \quad \Delta R = + 5.6 \text{ sec}$$

$$85^\circ \leq Z \leq 92^\circ \quad \Delta R = -14.7 \text{ sec}$$

$$92^\circ \leq Z \leq 93^\circ \quad \Delta R = -15.0 \text{ sec}$$

## VI. Refraction Model Functional Dependence Upon Pressure, Temperature, and Relative Humidity

It was originally felt that once a refraction model for standard conditions ( $P = 760$  mm and  $T = 0^\circ\text{C}$ ) had been achieved, the usual scaling by  $P/760$  and  $273/(T + 273)$  could be applied. However, after examining different combinations of  $P$  and  $T$  in the Garfinkel data, this did not prove to be an adequate treatment of the pressure and temperature dependence, and additional work in this area was required.

### A. Pressure Correction

Examination of the Garfinkel data at different pressures indicated that scaling of the basic model by  $P/760$  was reasonable at most  $Z$ , but broke down as  $Z \gtrsim 90^\circ$ . It was hoped that this could be compensated for by a correction factor (say,  $\Delta_1(P, Z)$ ) such that the entire pressure correction factor would be of the form:

$$\frac{P}{760} \{ 1 - \Delta_1(P, Z) \}$$

Furthermore, it would be necessary that:

$$\Delta_1(P, Z) \rightarrow 0, \quad Z \lesssim 90^\circ$$

$$\Delta_1(P, Z) \rightarrow 0, \quad Z \gtrsim 93^\circ$$

It was noted in the examination of the Garfinkel data that the pressure effect (as different from  $P/760$ ) was for the most part separable, i.e.:

$$\Delta_1(P, Z) \sim \Delta_p(P)\Delta_z(Z)$$

and it could be seen that further:

$$\Delta_p(P) \sim (P - 760)$$

A representation for  $\Delta_z$  was then empirically constructed as follows:

$$\Delta_z(Z) \sim \exp [A_1(Z - A_2)]$$

so that the  $\Delta_1(P, Z)$  pressure correction would be:

$$\Delta_1(P, Z) = (P - 760) \exp [A_1(Z - A_2)]$$

The results of using  $\Delta_1(P, Z)$ , above, can be seen in Fig. 9. Finally, to satisfy the conditions of a small  $\Delta_1(P, Z)$  for  $Z \gtrsim 93^\circ$ , the previously determined  $\Delta_3(Z)$  was utilized to arrive at the following expression:

Pressure correction factor =

$$\frac{P}{760} \left\{ 1 - \frac{(P - 760) \exp [A_1(Z - A_2)]}{1 + \Delta_3(Z)} \right\}$$

where

$Z$  = zenith angle, deg

$P$  = pressure, mm of Hg

$$A_1 = 0.40816$$

$$A_2 = 112.30$$

$\Delta_3(Z)$  = as previously defined

## B. Temperature Correction

The investigation of temperature effects proceeded along the same lines as the investigation of pressure effects in the previous section, with the goal of a total temperature correction factor in the form of:

$$\frac{273}{T + 273} \{1 - \Delta_2(T, Z)\}$$

in combination with the conditions:

$$\Delta_2(T, Z) \rightarrow 0, \quad Z \lesssim 90^\circ$$

$$\Delta_2(T, Z) \rightarrow 0, \quad Z \gtrsim 93^\circ$$

Similarly, the temperature effect was found to be approximately separable:

$$\Delta_2(T, Z) \sim \Delta_t(T)\Delta_z(Z)$$

and the following was (empirically) constructed:

$$\Delta_t \sim T$$

$$\Delta_z \sim \exp [B_1(Z - B_2)]$$

so that the  $\Delta_2(T, Z)$  temperature correction would be:

$$\Delta_2(T, Z) = (T) \exp [B_1(Z - B_2)]$$

The results of using  $\Delta_2(T, Z)$ , above, are seen in Fig. 10. Once again, to satisfy the condition of a small  $\Delta_2(T, Z)$  for  $Z \gtrsim 93^\circ$ , the previously determined  $\Delta_3(Z)$  is utilized to arrive at the following total expression:

Temperature correction factor =

$$\frac{273}{T + 273} \left\{ 1 - \frac{(T) \exp [B_1(Z - B_2)]}{1 + \Delta_3(Z)} \right\}$$

where

$Z$  = zenith angle, deg

$T$  = temperature, °C

$$B_1 = 0.12820$$

$$B_2 = 142.88$$

$\Delta_3(Z)$  = as previously determined

## C. Relative Humidity Correction

Both the Garfinkel (see Ref. 2) and the Pulkova models (see Ref. 4) indicate that the correction for relative humidity is very small, perhaps on the order of several seconds, at large  $Z$ . This seems reasonable since optical refraction is generally considered to be proportional to dry refractivity:

$$R = R_{\text{optical}} \sim N_{\text{dry}}$$

where

$$N_{\text{dry}} \cong 77.6 \left\{ \frac{P}{T} \right\}$$

whereas radio frequency refraction is considered to be proportional to total refractivity:

$$R_{\text{radio}} \sim N_{\text{dry}} + N_{\text{wet}} \\ \sim N_{\text{dry}} \left\{ 1 + \frac{N_{\text{wet}}}{N_{\text{dry}}} \right\}$$

where

$$N_{\text{wet}} \cong 77.6 [4810] \left\{ \frac{(RH) e_s(T)}{T^2} \right\}$$

and

$RH$  = relative humidity

$e_s$  = saturation vapor pressure

If one should merely account for this difference by scaling the optical results by the following factor (as is effectively what has been done in the past):

$$\left\{ 1 + \frac{N_{\text{wet}}}{N_{\text{dry}}} \right\}$$

so that:

$$R_{\text{radio}}(P, T, RH, Z) \cong R_{\text{optical}}(P, T, Z) \left\{ 1 + \frac{N_{\text{wet}}}{N_{\text{dry}}} \right\}$$

one would immediately expect the transformed model ( $R_{\text{radio}}$ ) to preserve the design features from Section II as well as to possess considerably greater accuracy than the current JPL models. However, the whole question of transforming the optical angular refraction model described in this report to the radio frequency level requires additional study before a definitive statement about the transformed model accuracies can be made.

## VII. Complete Angular Refraction With Pressure and Temperature Corrections

The final refraction model with pressure and temperature accounted for is as follows:

$$R = F_p F_t \left( \exp \left\{ \frac{\sum_{j=0}^8 K_{j+3} [U(Z)]^j}{1 + \Delta_3(Z)} \right\} - K_{12} \right) \\ F_p = \left( \frac{P}{P_0} \left\{ 1 - \frac{\Delta_1(P, Z)}{1 + \Delta_3(Z)} \right\} \right)$$

$$F_t = \left( \frac{T_0}{T} \left\{ 1 - \frac{\Delta_2(T, Z)}{1 + \Delta_3(Z)} \right\} \right)$$

$$\Delta_1(P, Z) = (P - P_0) \{ \exp [A_1(Z - A_2)] \}$$

$$\Delta_2(T, Z) = (T - T_0) \{ \exp [B_1(Z - B_2)] \}$$

$$\Delta_3(Z) = (Z - C_0) \{ \exp [C_1(Z - C_2)] \}$$

where

$R$  = refraction, sec

$Z$  = actual zenith angle, deg

$EL = 90^\circ - Z$  = elevation angle

$$U(Z) = \left\{ \frac{Z - K_1}{K_2} \right\}$$

$$K_1 = 46.625$$

$$K_2 = 45.375$$

$$K_3 = 4.1572$$

$$K_4 = 1.4468$$

$$K_5 = 0.25391$$

$$K_6 = 2.2716$$

$$K_7 = 1.3465$$

$$K_8 = -4.3877$$

$$K_9 = 3.1484$$

$$K_{10} = 4.5201$$

$$K_{11} = -1.8982$$

$$K_{12} = 0.89000$$

$P$  = pressure, mm of Hg

$$P_0 = 760.00 \text{ mm}$$

$$A_1 = 0.40816$$

$$A_2 = 112.30$$

$T$  = temperature, K

$$T_0 = 273.00 \text{ K}$$

$$B_1 = 0.12820$$

$$B_2 = 142.88$$

$$C_0 = 91.870$$

$$C_1 = 0.80000$$

$$C_2 = 99.344$$

The accuracy of this model for various pressures, temperatures, and ranges of  $Z$ , as compared to the Garfinkel data, can be seen in Table 2.

The signature of the residuals at large  $Z$  and with  $P = 760$  mm and  $T = 0^\circ\text{C}$  can be seen in Fig. 7 (modified 8th order  $\ln R$  fit). For use where simplicity is of a more urgent need than accuracy, an abbreviated version of the model can be obtained by setting:

$$\Delta_1 = \Delta_2 = \Delta_3 = 0$$

such that one has:

$$R = \left(\frac{P}{P_0}\right) \left(\frac{T_0}{T}\right) \left(\exp \left\{ \sum_{j=0}^8 K_{j+3} [U(Z)]^j \right\} - K_{12} \right)$$

where all quantities are as previously defined. The accuracy of this abbreviated version, once again as compared to the Garfinkel data, is seen in Table 3. Also, the effects of the deletion of  $\Delta_1$  is seen in Fig. 9, of  $\Delta_2$  in Fig. 10, and of  $\Delta_3$  in Fig. 7.

## VIII. FORTRAN Subroutines of the Refraction Models

Appendix A presents a FORTRAN subroutine of the full model described in Section VII, while Appendix B presents a FORTRAN subroutine corresponding to the

abbreviated model, also described in Section VII. Inputs required are as follows:

PRESS = pressure, mm of Hg

TEMP = temperature, K

ZNITH = actual zenith angle, deg

and the subroutine(s) return with:

$R$  = refraction correction, sec

## IX. Summary

An empirical model has been constructed which very accurately reflects precise optical refraction data. The salient features possessed by this model are as follows:

- (1) Single analytic function.
- (2) Finite over the entire domain of elevation angle.
- (3) High accuracy for large ranges of pressure and temperatures.
- (4) Designed to minimize computer storage and run time.

For S- and X-band applications, the model must be transformed from optical frequencies to radio frequencies. It is hoped that by considering the differences in optical refractivity versus radio frequency refractivity, a reasonably accurate method of transforming optical refraction to radio frequency refraction can be found.

## References

1. Garfinkel, B., "An Investigation in the Theory of Astronomical Refraction," *Astron. J.*, Vol. 50, No. 8, 1944.
2. Garfinkel, B., "Astronomical Refraction in a Polytrropic Atmosphere," *Astron J.*, Vol. 72, No. 2, 1967.
3. Mueller, I. I., *Spherical and Practical Astronomy as Applied to Geodesy*, Frederick Ungar Publishing Co., New York, 1969.
4. Orlov, B. A., *Refraction Tables of Pulkova Observatory*, 4th Edition, 1956.
5. Lawson, C. L., "Least Squares Polynomial Fit to Data, S.P.," *JPL Fortran V Subroutine Directory*, 1846-23 (JPL internal document).



## Bibliography

- Berman, A. L., *Adjustment of Predict Refraction Model to Prevent (Apparent) Lagrangian Interpolation Problems in Angle Predictions*, 401-2177, Aug. 13, 1971 (JPL internal document).
- Rovello, R. C., *Antenna Pointing Subsystem Phase I, Computer Program, DSIF 210 ft Antennas*, 900-22, 315-R-6, Rev. 1, June 1967 (JPL internal document).
- Smart, W. M., *Spherical Astronomy*, Cambridge University Press, London, 1965.

**Table 1. Garfinkel refraction data<sup>a</sup> for  
P = 760 mm and T = 0°C**

Z	R	R'	Z	R	R'
0.0	0.00	0.00	22.5	25.09	25.09
0.5	0.55	0.55	23.0	25.71	25.72
1.0	1.07	1.08	23.5	26.33	26.34
1.5	1.61	1.61	24.0	26.97	26.97
2.0	2.15	2.15	24.5	27.60	27.61
2.5	2.68	2.68	25.0	28.25	28.26
3.0	3.22	3.22	25.5	28.90	28.91
3.5	3.75	3.76	26.0	29.55	29.56
4.0	4.29	4.29	26.5	30.21	30.22
4.5	4.83	4.83	27.0	30.88	30.89
5.0	5.36	5.36	27.5	31.55	31.56
5.5	5.90	5.90	28.0	32.23	32.24
6.0	6.43	6.44	28.5	32.91	32.92
6.5	6.97	6.97	29.0	33.60	33.62
7.0	7.51	7.51	29.5	34.30	34.32
7.5	8.05	8.05	30.0	35.01	35.02
8.0	8.59	8.59	30.5	35.72	35.73
8.5	9.12	9.13	31.0	36.43	36.45
9.0	9.67	9.67	31.5	37.16	37.17
9.5	10.21	10.21	32.0	37.89	37.91
10.0	10.75	10.75	32.5	38.63	38.65
10.5	11.30	11.30	33.0	39.38	39.40
11.0	11.84	11.84	33.5	40.14	40.16
11.5	12.39	12.39	34.0	40.90	40.92
12.0	12.94	12.94	34.5	41.68	41.70
12.5	13.49	13.49	35.0	42.46	42.48
13.0	14.04	14.05	35.5	43.26	43.27
13.5	14.60	14.60	36.0	44.06	44.08
14.0	15.15	15.16	36.5	44.87	44.89
14.5	15.71	15.72	37.0	45.69	45.71
15.0	16.28	16.28	37.5	46.53	46.55
15.5	16.84	16.85	38.0	47.37	47.39
16.0	17.41	17.41	38.5	48.23	48.25
16.5	17.98	17.98	39.0	49.10	49.12
17.0	18.55	18.56	39.5	49.98	50.00
17.5	19.13	19.13	40.0	50.87	50.89
18.0	19.70	19.71	40.5	51.77	51.80
18.5	20.29	20.29	41.0	52.69	52.72
19.0	20.87	20.88	41.5	53.62	53.65
19.5	21.46	21.47	42.0	54.56	54.59
20.0	22.06	22.06	42.5	55.52	55.55
20.5	22.65	22.66	43.0	56.50	56.53
21.0	23.26	23.66	43.5	57.49	57.52
21.5	23.86	23.87	44.0	58.50	58.53
22.0	24.47	24.48	44.5	59.52	59.56

<sup>a</sup>R gives the refraction correction if Z = actual while R' gives the refraction correction if Z = observed.

**Table 1 (contd)**

Z	R	R'	Z	R	R'
45.0	60.56	60.60	69.0	156.61	156.97
45.5	61.63	61.67	69.5	160.75	161.13
46.0	62.72	62.76	70.0	165.06	165.46
46.5	63.83	63.87	70.2	166.83	167.25
47.0	64.95	64.99	70.4	168.63	169.06
47.5	66.10	66.15	70.6	170.47	170.91
48.0	67.28	67.32	70.8	172.33	172.78
48.5	68.47	68.52	71.0	174.23	174.69
49.0	69.69	69.73	71.2	176.16	176.64
49.5	70.93	70.97	71.4	178.13	178.63
50.0	72.19	72.24	71.6	180.15	180.66
50.5	73.48	73.53	71.8	182.20	182.73
51.0	74.79	74.85	72.0	184.30	184.85
51.5	76.14	76.19	72.2	186.44	187.01
52.0	77.51	77.57	72.4	188.64	189.23
52.5	78.91	78.97	72.6	190.90	191.51
53.0	80.34	80.40	72.8	193.21	193.84
53.5	81.80	81.87	73.0	195.57	196.22
54.0	83.30	83.37	73.2	197.97	198.64
54.5	84.83	84.91	73.4	200.41	201.10
55.0	86.40	86.48	73.6	202.90	203.62
55.5	88.02	88.10	73.8	205.45	206.19
56.0	89.68	89.77	74.0	208.07	208.84
56.5	91.39	91.48	74.2	210.75	211.56
57.0	93.14	93.23	74.4	213.51	214.35
57.5	94.94	95.03	74.6	216.34	217.20
58.0	96.78	96.88	74.8	219.23	220.12
58.5	98.67	98.78	75.0	222.18	223.11
59.0	100.61	100.72	75.2	225.21	226.18
59.5	102.61	102.72	75.4	228.33	229.34
60.0	104.66	104.78	75.6	231.54	232.60
60.5	106.76	106.89	75.8	234.84	235.94
61.0	108.93	109.06	76.0	238.20	239.34
61.5	111.17	111.31	76.2	241.64	242.81
62.0	113.49	113.64	76.4	245.15	246.37
62.5	115.93	116.10	76.6	248.77	250.05
63.0	118.47	118.64	76.8	252.50	253.85
63.5	121.10	121.28	77.0	256.35	257.75
64.0	123.79	123.98	77.2	260.29	261.74
64.5	126.53	126.72	77.4	264.33	265.85
65.0	129.35	129.56	77.6	268.50	270.10
65.5	132.28	132.50	77.8	272.80	274.48
66.0	135.33	135.57	78.0	277.24	279.00
66.5	138.51	138.76	78.2	281.80	283.63
67.0	141.82	142.09	78.4	286.49	288.41
67.5	145.26	145.55	78.6	291.32	293.34
68.0	148.86	149.17	78.8	296.33	298.45
68.5	152.64	152.97	79.0	301.50	303.73

Table 1 (contd)

Z	R	R'	Z	R	R'
79.2	306.85	309.20	86.9	842.56	885.73
79.4	312.36	314.82	87.0	859.68	905.41
79.6	318.03	320.62	87.1	877.38	925.93
79.8	323.92	326.68	87.2	895.71	947.24
80.0	330.09	333.02	87.3	914.73	969.38
80.2	336.46	339.52	87.4	934.45	992.51
80.4	342.99	346.20	87.5	954.84	1016.58
80.6	349.75	353.18	87.6	975.96	1041.62
80.8	356.81	360.45	87.7	997.91	1067.68
81.0	364.17	368.05	87.8	1020.64	1095.01
81.2	371.82	375.93	87.9	1044.16	1123.53
81.4	379.76	384.12	88.0	1068.53	1153.28
81.6	387.99	392.61	88.1	1093.93	1184.47
81.8	396.55	401.48	88.2	1120.27	1217.10
82.0	405.48	410.74	88.3	1147.59	1251.29
82.2	414.76	420.35	88.4	1176.01	1287.15
82.4	424.44	430.45	88.5	1205.55	1324.68
82.6	434.59	441.05	88.6	1236.25	1364.16
82.8	445.21	452.12	88.7	1268.19	1405.55
83.0	456.30	463.71	88.8	1301.38	1449.01
83.2	467.87	475.82	88.9	1335.90	1494.78
83.4	480.03	488.71	89.0	1371.84	1543.13
83.6	492.90	502.21	89.1	1409.18	1594.01
83.8	506.32	516.28	89.2	1448.01	1647.64
84.0	520.31	531.10	89.3	1488.47	1704.25
84.2	535.04	546.76	89.4	1530.70	1764.12
84.4	550.57	563.28	89.5	1574.66	1827.44
84.6	566.91	580.76	89.6	1620.40	1894.34
84.8	584.18	599.35	89.7	1668.02	1965.25
85.0	602.50	619.11	89.8	1717.65	2040.56
85.1	612.07	629.38	89.9	1769.36	2123.12
85.2	621.88	639.99	90.0	1823.24	2205.54
85.3	631.94	650.89	90.1	1879.28	2298.34
85.4	642.32	662.10	90.2	1937.63	2392.18
85.5	652.95	673.70	90.3	1998.35	2495.00
85.6	663.88	685.73	90.4	2062.49	2604.75
85.7	675.18	698.15	90.5	2130.07	2722.08
85.8	686.86	710.99	90.6	2196.81	2847.58
85.9	698.89	724.30	90.7	2269.53	2982.06
86.0	711.31	738.00	90.8	2343.68	3126.84
86.1	724.15	752.11	90.9	2419.93	3282.69
86.2	737.33	766.87	91.0	2500.71	3450.46
86.3	750.87	782.12	91.1	2584.52	3632.11
86.4	764.99	797.78	91.2	2671.66	3827.51
86.5	779.57	814.09	91.3	2762.19	4039.04
86.6	794.50	831.04	91.4	2856.17	4269.13
86.7	809.95	848.62	91.5	2953.70	4519.72
86.8	825.98	866.83	91.6	3055.07	4792.26

Table 1 (contd)

Z	R	R'	Z	R	R'
91.7	3160.32	5090.87	92.4	4009.10	8246.36
91.8	3269.46	5418.31	92.5	4147.07	8926.70
91.9	3382.48	5777.87	92.6	4289.48	9692.48
92.0	3499.59	6174.23	92.7	4436.33	10560.24
92.1	3621.06	6612.15	92.8	4587.50	11551.26
92.2	3746.26	7097.56	92.9	4742.84	12684.70
92.3	3875.53	7638.78	93.0	4902.77	13986.89

Table 2. Maximum refraction model residuals for selected P, T, and ranges of Z

Temperature, °C	Maximum refraction model residuals, sec		
	P = 700	P = 760	P = 800
a. $0^\circ \leq Z \leq 85^\circ$			
-10	+4.59	+4.87	+5.05
0	+5.25	+5.59	+5.82
+10	+5.83	+6.24	+6.51
+20	+6.41	+6.88	+7.18
+30	+6.98	+7.50	+7.83
b. $85^\circ \leq Z < 93^\circ$			
-10	-15.41	-18.36	-24.30
0	-13.56	-15.03	-17.45
+10	-11.91	-14.27	-14.02
+20	-15.16	-14.77	-12.61
+30	-19.20	-16.20	+13.94

Table 3. Maximum refraction model residuals for selected P, T, and ranges of Z:  $\Delta_1, \Delta_2, \Delta_3 = 0$ 

Temperature, °C	Maximum refraction model residuals, sec		
	P = 700	P = 760	P = 800
a. $0^\circ \leq Z \leq 85^\circ$			
-10	+6.06	+6.38	+6.57
0	+5.33	+5.61	+5.78
+10	+4.68	+4.93	+5.08
+20	+4.11	+4.32	+4.45
+30	+3.59	-5.41	-6.06
b. $85^\circ \leq Z < 93^\circ$			
-10	+102.05	-188.07	-278.89
0	-130.49	-251.98	-338.33
+10	-196.42	-312.90	-395.56
+20	-258.65	-370.69	-450.09
+30	-317.28	-452.40	-501.90

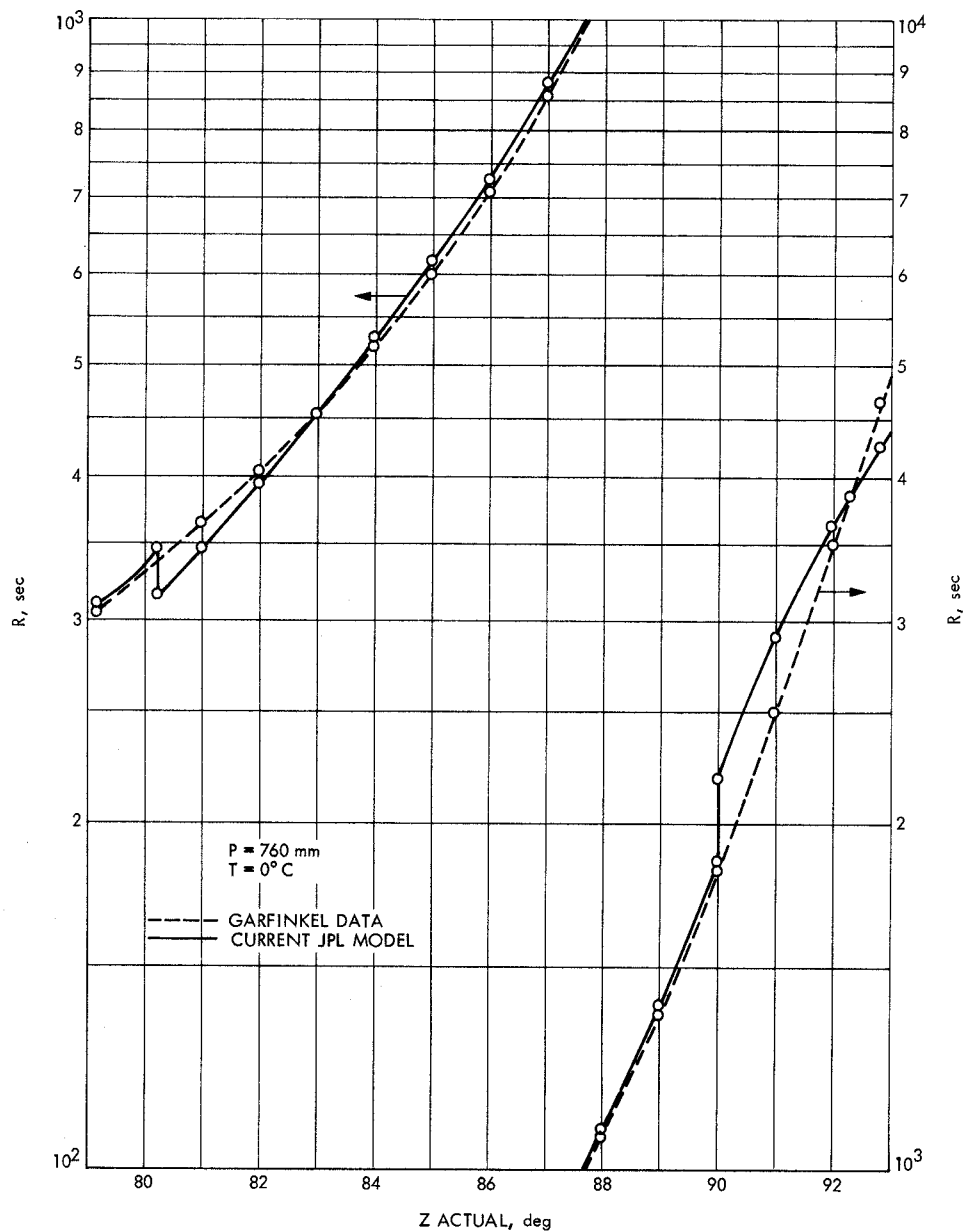


Fig. 1. Current 3-segment JPL angular refraction model versus Garfinkel refraction data

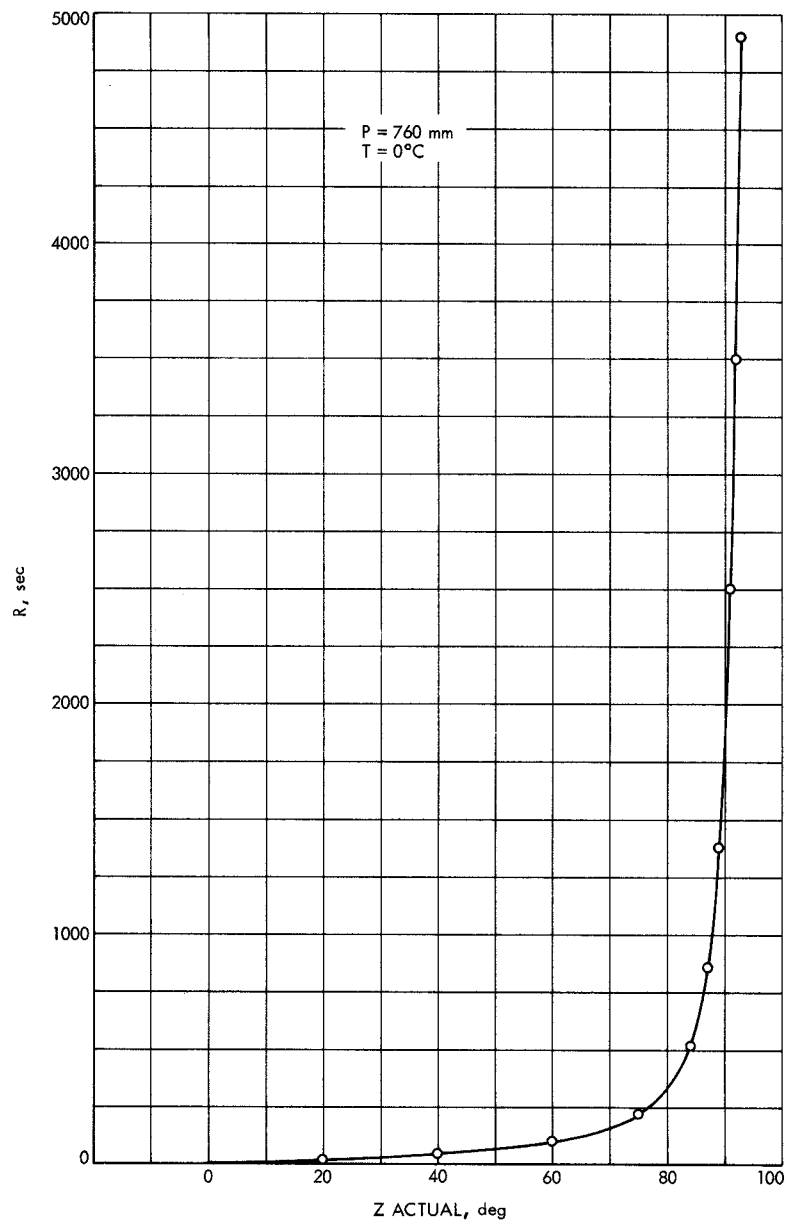


Fig. 2. Garfinkel refraction data

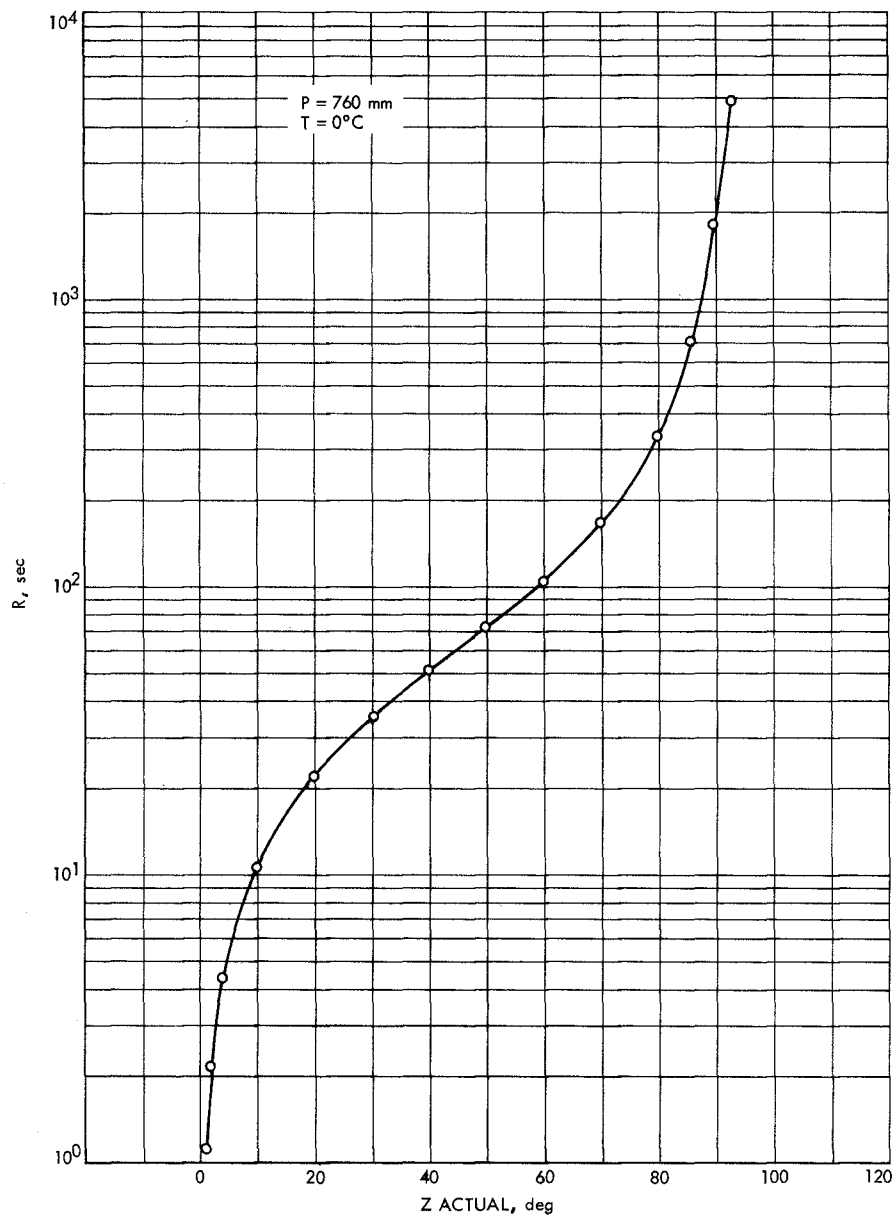


Fig. 3. Garfinkel refraction data (logarithmic)

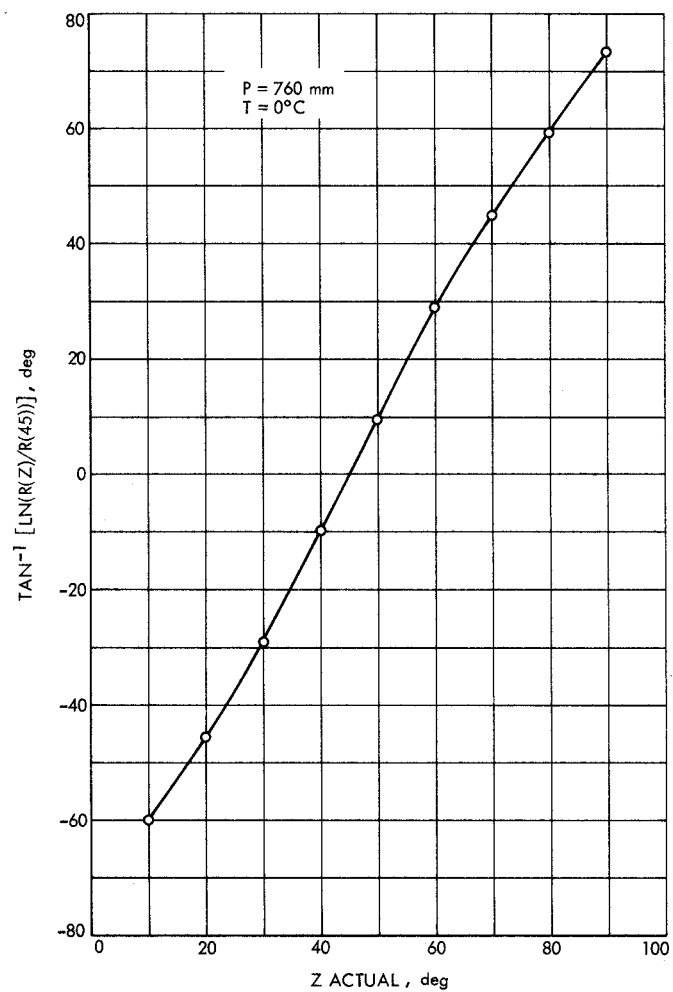


Fig. 4. Garfinkel refraction data ( $\arctan (\ln R)$ )

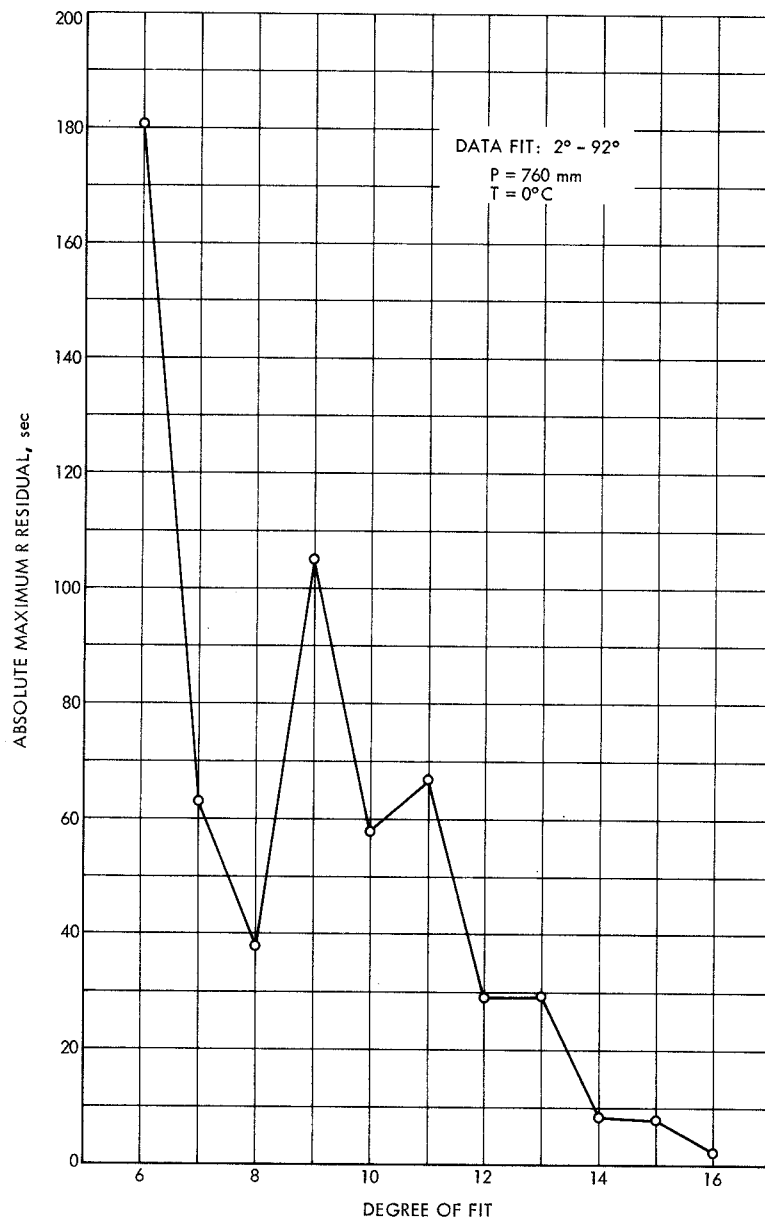


Fig. 5. Least squares fit of  $\ln R$  (Garfinkel data) to an  $n$ th degree polynomial



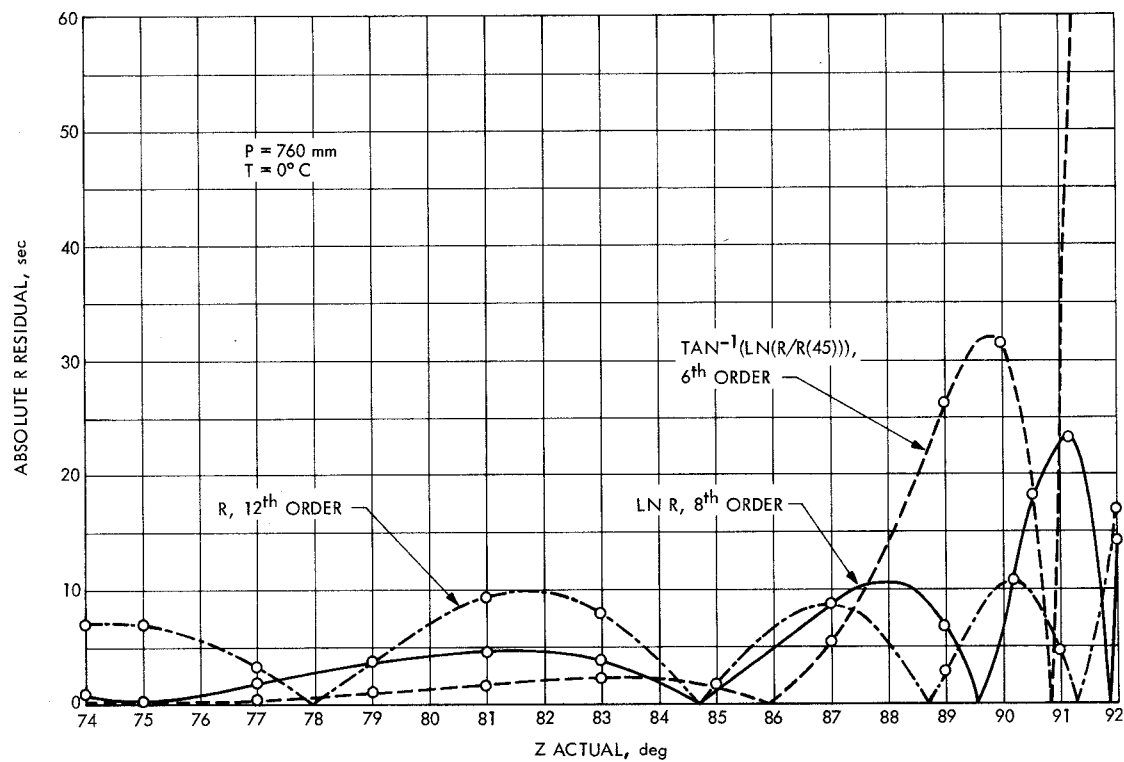


Fig. 6. Various functional forms of  $R$  fit to an  $n$ th degree polynomial

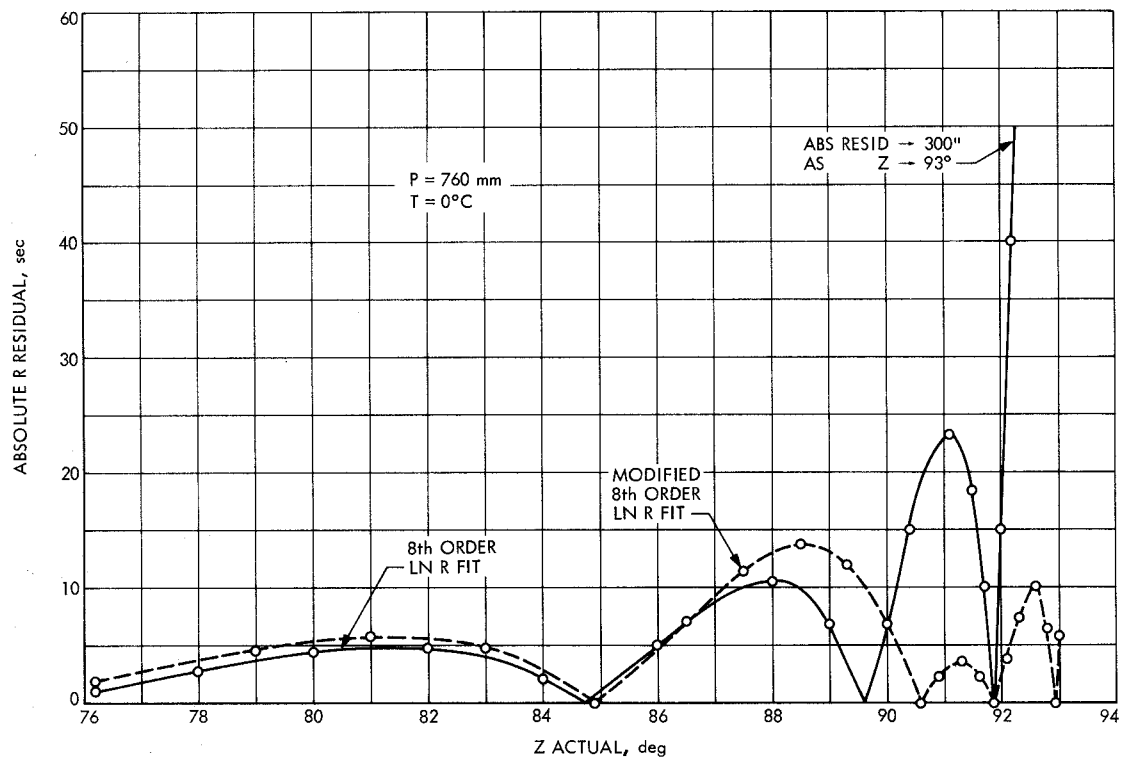


Fig. 7. 8th degree and modified 8th degree polynomial fit to  $\ln R$  (Garfinkel data)

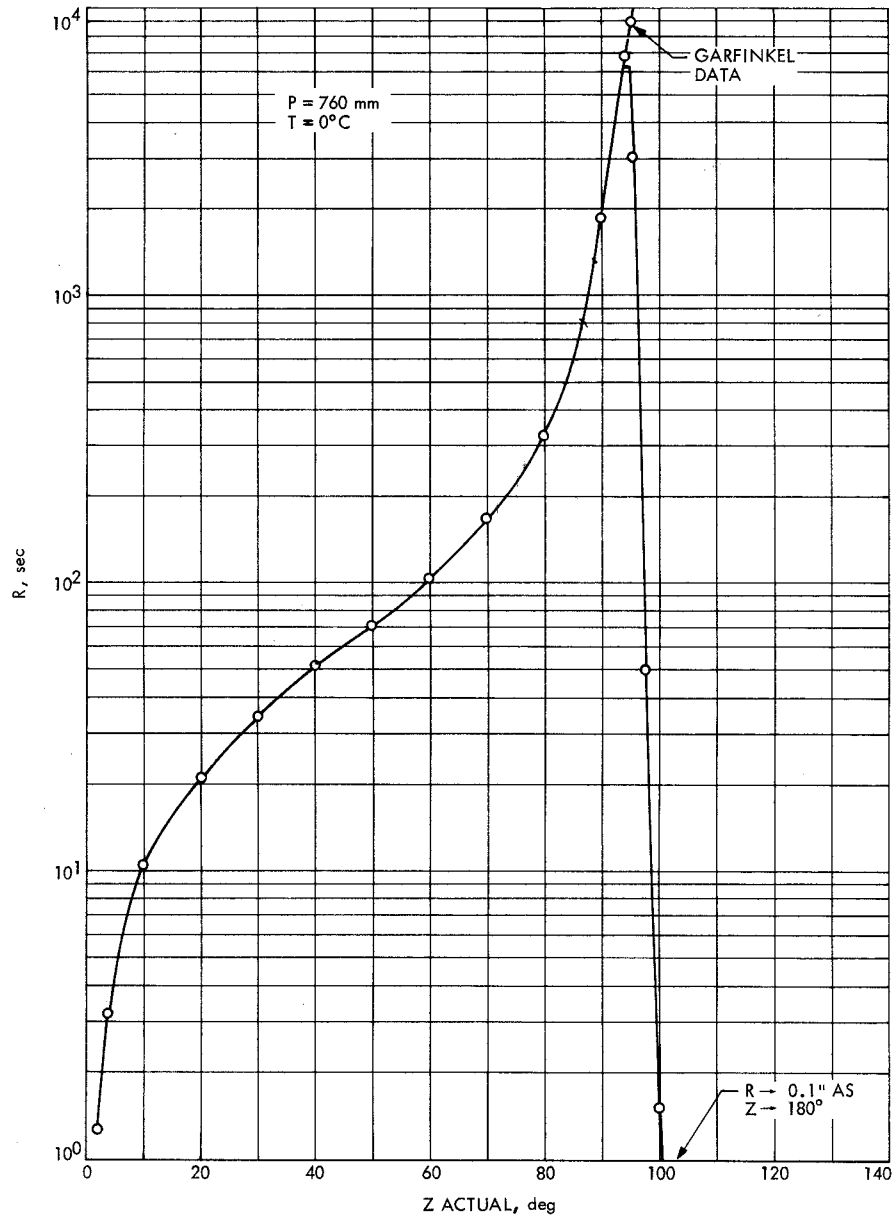


Fig. 8. Berman-Rockwell refraction model

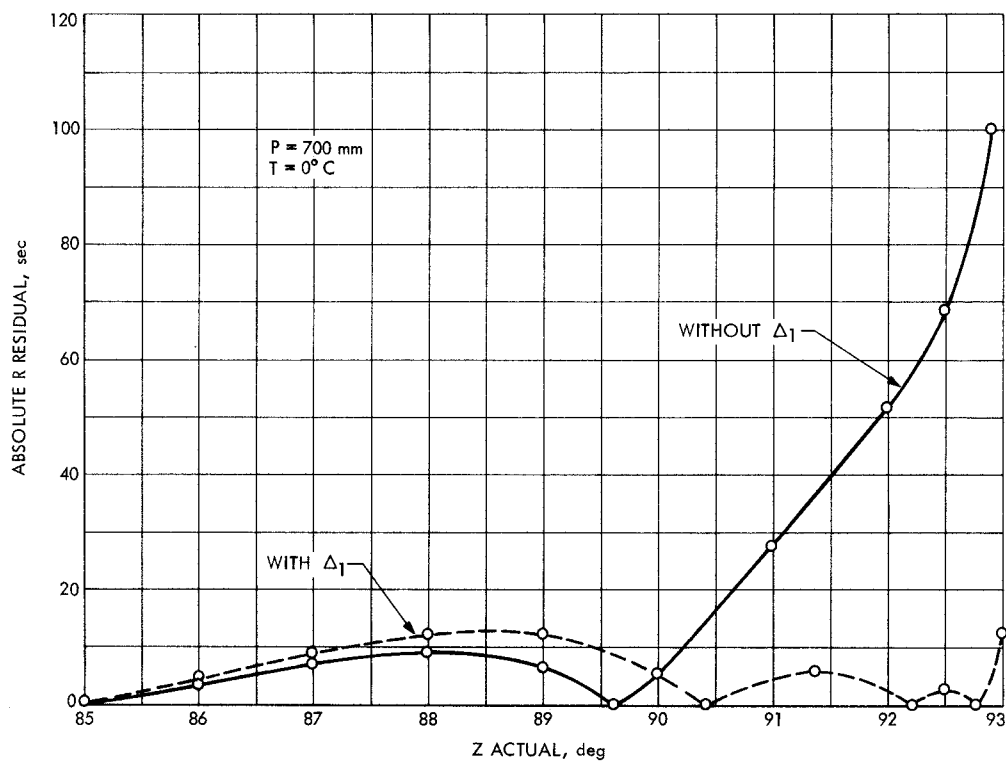


Fig. 9. Refraction model with and without  $\Delta_1$  (pressure correction factor)

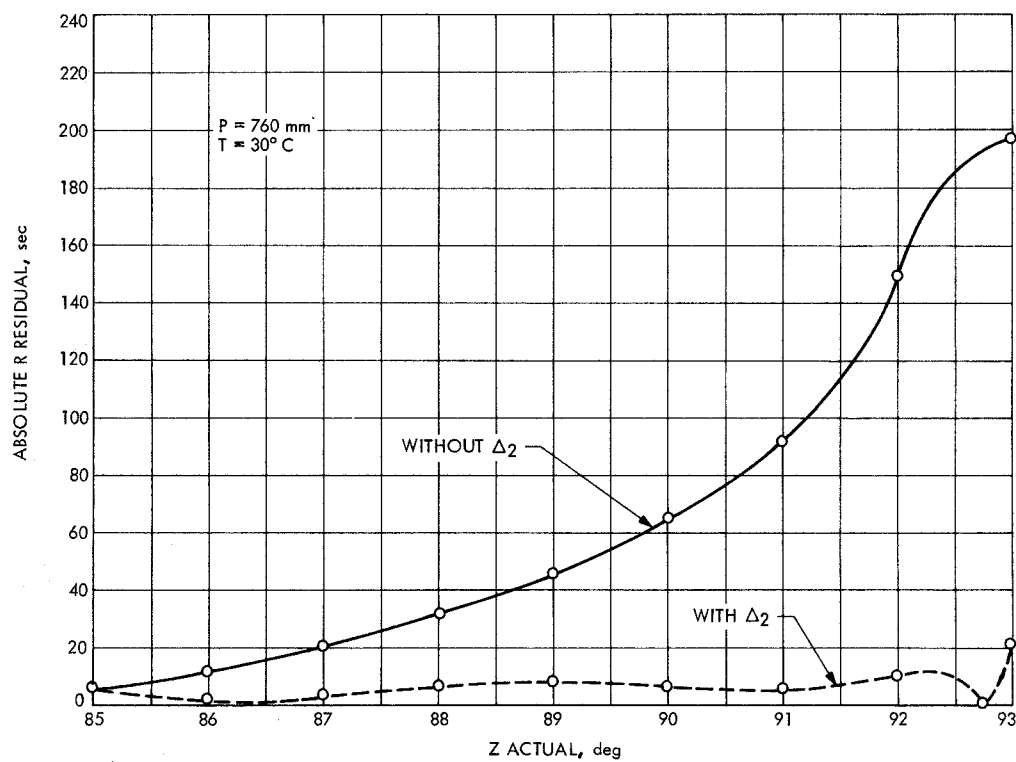


Fig. 10. Refraction model with and without  $\Delta_2$  (temperature correction factor)

## Appendix A

```

00101      1*      SUBROUTINE BEND(PRESS,TEMP,ZNITH,R)
00103      2*      DIMENSION A(2),B(2),C(2),E(12),P(2),T(2),Z(2)
00104      3*      P(1) = 760.00
00105      4*      P(2) = PRESS
00106      5*      T(1) = 273.00
00107      6*      T(2) = TEMP
00110      7*      Z(1) = 91.870
00111      8*      Z(2) = ZNITH
00112      9*      A(1) = .40816
00113     10*      A(2) = 112.30
00114     11*      B(1) = .12820
00115     12*      B(2) = 142.88
00116     13*      C(1) = .80000
00117     14*      C(2) = 99.344
00120     15*      E(1) = 46.625
00121     16*      E(2) = 45.375
00122     17*      E(3) = 4.1572
00123     18*      E(4) = 1.4468
00124     19*      E(5) = .25391
00125     20*      E(6) = 2.2716
00126     21*      E(7) = -1.3465
00127     22*      E(8) = -4.3877
00130     23*      E(9) = 3.1484
00131     24*      E(10) = 4.5201
00132     25*      E(11) = -1.8982
00133     26*      E(12) = .89000
00134     27*      D3=1.+DELTA(Z,C,Z(2))
00135     28*      FP=(P(2)/P(1))*(1.-DELTA(P,A,Z(2))/D3)
00136     29*      FT=(T(1)/T(2))*(1.-DELTA(T,B,Z(2))/D3)
00137     30*      U=(Z(2)-E(1))/E(2)
00140     31*      X=E(11)
00141     32*      DO 1 I=1,8
00144     33*      1 X=E(11-I)+U*X
00146     34*      R=FT*FP*(EXP(X/D3)-E(12))
00147     35*      RETURN
00150     36*      END

```

```

00101      1*      FUNCTION DELTA(A,B,Z)
00103      2*      DIMENSION A(2),B(2)
00104      3*      DELTA=(A(2)-A(1))*EXP(B(1)*(Z-B(2)))
00105      4*      RETURN
00106      5*      END

```

## Appendix B

00101	1*	SUBROUTINE BEND(PRESS,TEMP,ZNITH,R)
00103	2*	DIMENSION E(12)
00104	3*	P = 760.00
00105	4*	T = 273.00
00106	5*	E(1) = 46.625
00107	6*	E(2) = 45.375
00110	7*	E(3) = 4.1572
00111	8*	E(4) = 1.4468
00112	9*	E(5) = .25391
00113	10*	E(6) = 2.2716
00114	11*	E(7) = -1.3465
00115	12*	E(8) = -4.3877
00116	13*	E(9) = 3.1484
00117	14*	E(10) = 4.5201
00120	15*	E(11) = -1.8982
00121	16*	E(12) = .89000
00122	17*	FP=PRESS/P
00123	18*	FT=T/TEMP
00124	19*	U=(ZNITH-E(1))/E(2)
00125	20*	X=E(11)
00126	21*	DO 1 I=1,8
00131	22*	1 X=E(11-I)+U*X
00133	23*	R=FT*FP*(EXP(X)-E(12))
00134	24*	RETURN
00135	25*	END